Fermi Arcs in the Superconducting Clustered State for Underdoped Cuprate Superconductors

G. Alvarez

Computer Science & Mathematics Division and Center for Nanophase Materials Sciences, Oak Ridge National Laboratory, Oak Ridge, Tennessee 37831, USA

E. Dagotto

Department of Physics and Astronomy, University of Tennessee, Knoxville, Tennessee 37996, USA, and Materials Science and Technology Division, Oak Ridge National Laboratory, Oak Ridge, Tennessee 32831, USA

(Received 1 February 2008; published 23 October 2008)

The one-particle spectral function of a state formed by superconducting (SC) clusters is studied via Monte Carlo techniques. The clusters have similar SC amplitudes but randomly distributed phases. This state is stabilized by competition with the antiferromagnetism expected to be present in the cuprates and after quenched disorder is introduced. A Fermi surface composed of disconnected segments, i.e., Fermi arcs, is observed between the critical temperature T_c and the cluster formation temperature scale T^*.

DOI: 10.1103/PhysRevLett.101.177001 PACS numbers: 74.72.−h, 74.20.De, 74.20.Rp, 74.25.Jb

Introduction.—Research in hole-doped high temperature superconductors is currently mainly focusing on the pseudogap (PG) phase that exists above T_c in the underdoped regime. This exotic phase, with a depleted density of states at the chemical potential, acts as the normal state to superconductivity in a broad range of hole densities. Experiments have recently provided important microscopic information about the PG phase. (i) Using angle-resolved photoemission (ARPES) techniques [1], the PG Fermi surface was found to be composed of disconnected segments, widely known as ''Fermi arcs'' [2], that are centered at the nodal (N) points $\mathbf{k} = (\pm\pi/2, \pm\pi/2)$ of the low-temperature d-wave superconductor, in the two-dimensional (2D) square-lattice notation. These arcs are caused by the low-energy PG that presents a $\mathbf{k}$-dependence resembling a d-wave SC gap close to the antinodal (AN) points $(0, \pm\pi)$, $(\pm\pi, 0)$ [1], where the SC gap is the largest, but it has gapless excitations in a finite momentum range near the nodes [3,4]. The AN gaps remain approximately constant in the PG phase, in contrast with BCS calculations [3,4]. (ii) Using scanning tunneling microscopy (STM) techniques [5] and at temperatures above T_c, the local density-of-state (LDOS) still closely resembles that of a d-wave superconductor, namely, it has a linearly growing value away from the location of the chemical potential followed by peaks that define the gap. At optimal doping and $T = 120\,\mathrm{K} > T_c$, a d-wave gap is still observed in randomly distributed clusters [6].

Theoretically, the PG state is believed to be either (i) a precursor of the SC state, with phase fluctuations destroying superconductivity in an homogeneous state made out of small size Cooper pairs formed by a strong attraction [7], or (ii) caused by other competing orders. However, within the phase fluctuations context, another possibility was recently proposed [8]. Via Landau-Ginzburg (LG) calculations, a state with nanoscale SC and antiferromagnetic (AF) clusters is stabilized when quenched disorder (caused, e.g., by the random nature of chemical doping) influences on an otherwise homogeneous state with local coexistence of the SC and AF order parameters. At small length scales, the disorder favors AF or SC, unbalancing locally the near degeneracy of these competing states, causing the homogeneity to be lost. The SC amplitude is approximately the same in all the SC clusters. However, the SC order parameter phase, while uniform within each SC cluster, randomly changes from cluster to cluster causing the overall state to become non-SC. The competition with AF, supplemented by disorder, is needed for the SC clusters to form and, once formed, phase fluctuations between clusters, occurring even in a weak-coupling BCS regime, destroy the SC condensate. This ''Superconducting Clustered State'' (SCCS) accounts for the STM experiments [5] since both are based on a similar inhomogeneous distribution of SC gaps above T_c. Here, we continue the analysis of the SCCS showing that this state also produces a Fermi surface (FS) with Fermi arcs, a quite unexpected result.

LG simulations.—Our calculations start with a LG theory for the AF vs d-wave SC competition, studied with Monte Carlo (MC) techniques. Details were extensively discussed before [8]. The LG classical Hamiltonian involves a complex number $\Delta_\mathbf{i} = |\Delta_\mathbf{i}|e^{i\phi_\mathbf{i}}$ and a real vector $\mathbf{S_i}$, representing the SC and AF order parameters at site $\mathbf{i}$ of a 2D square lattice. These two order parameters are dominant in the cuprates, and any minimal theory must incorporate them. The interactions are the standard: 1. terms with up to 4th powers of the order parameters, locally favoring SC and AF; 2. nearest-neighbor (NN) couplings that spread the range of the order, emerging from gradients in the continuum formulation; and 3. an interaction between the order parameters, with strength $u_{\mathrm{SC|AF}}$. Quenched disorder is also included to represent chemically

doped cuprates. More specifically,

$$H = r_{\mathrm{SC}}\sum_{\mathbf{i}}|\Delta_{\mathbf{i}}|^2 + \frac{u_{\mathrm{SC}}}{2}\sum_{\mathbf{i}}|\Delta_{\mathbf{i}}|^4 + \sum_{\mathbf{i},\alpha}\rho_{\mathrm{AF}}(\mathbf{i},\alpha)\mathbf{S}_{\mathbf{i}}\cdot\mathbf{S}_{\mathbf{i}+\alpha} + \sum_{\mathbf{i},\alpha}\rho_{\mathrm{SC}}(\mathbf{i},\alpha)|\Delta_{\mathbf{i}}||\Delta_{\mathbf{i}+\alpha}|\cos(\phi_{\mathbf{i}}-\phi_{\mathbf{i}+\alpha}) + r_{\mathrm{AF}}\sum_{\mathbf{i}}|\mathbf{S}_{\mathbf{i}}|^2 + \frac{u_{\mathrm{AF}}}{2}\sum_{\mathbf{i}}|\mathbf{S}_{\mathbf{i}}|^4 + u_{\mathrm{SC|AF}}\sum_{\mathbf{i}}|\Delta_{\mathbf{i}}|^2|\mathbf{S}_{\mathbf{i}}|^2. \quad (1)$$

Other on-site terms are excluded by symmetry. Previous investigations [8] showed that for a broad range of parameters [9] decreasing from zero the NN couplings ρ_{SC} (favoring SC) and simultaneously decreasing $\rho_{\mathrm{AF}} > 0$ (penalizing AF), e.g., along the line $\rho_{\mathrm{AF}} = 1 + \rho_{\mathrm{SC}}$, produces a clean-limit phase diagram with a SC + AF region of local coexistence. There is nothing special about the line $\rho_{\mathrm{AF}} = 1 + \rho_{\mathrm{SC}}$, which is here merely chosen for simplicity. Other interpolations from the AF to the SC states of Ref. [8] will lead to similar conclusions. Figure 1(a) qualitatively illustrates the clean-limit case ($D = 0$). However, quenched disorder $D \neq 0$, introduced in Eq. (1) via a random distribution of ρ_{SC} values (that affect ρ_{AF} as well, via their linear relation), reduces both critical temperatures, opening a gap between the competing phases. In this glassy region, nanoscale SC and AF clusters coexist [8] (see inset). Two temperature scales emerge naturally: upon cooling, first the SC inside a cluster develops at a crossover scale T^*, but the SC phases between clusters remain random. Reducing T further, coherence among the cluster phases is reached at T_c. The presence of two temperature scales is indeed observed numerically [Fig. 1(b)]. At $D = 0$, the long and short correlations are very similar, with T_c being defined as the T where the long-range correlation is, e.g., just 1% of the $T = 0$ result. At this T_c, the short-range correlation is about 17% of its maximum value. However, with disorder $D \neq 0$, a substantial difference between T_c (defined as before) and the T^* for short-range correlations (using the 17% criterion as in the clean limit) is clearly observed. Definitions based on other percentages do not alter the qualitative results. MC-equilibrated configurations of Eq. (1) better clarify this issue [Fig. 1(c)]. At low T, the uniform and intense color indicates a robust SC state. As T increases, phase fluctuations appear near T_c. In the interesting range $T_c < T < T^*$, both SC clusters with random phases and non-SC (white) regions coexist: this is the SCCS emphasized here [10]. Finally, near T^* or above, few vestiges of SC remain.

Fermions in the SC + AF *background.*—After LG/MC equilibrated configurations of the SCCS state are gathered, fermionic properties are obtained by locally coupling itinerant electrons (representing carriers of the doped cuprates) to the classical order parameters, as in [8]. In a mean-field spirit, these carriers are assumed to be moving in a static background given by the SC and AF order parameters. The Hamiltonian is

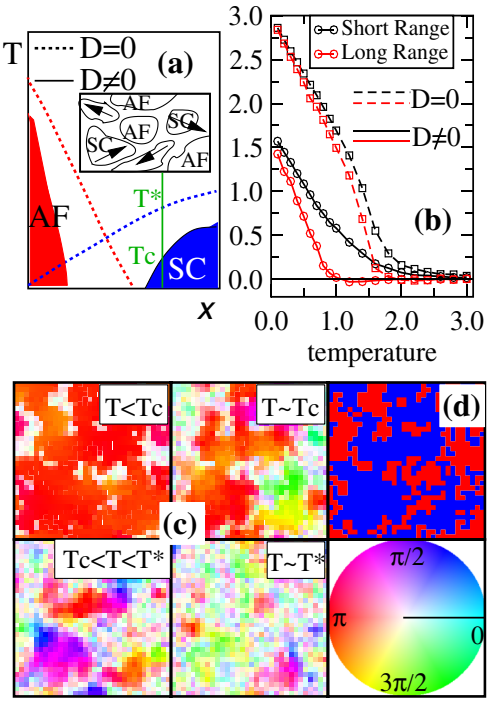

FIG. 1 (color online). (a) Schematic T vs doping (x) phase diagram [8] for the competition AF vs SC: $D = 0$ ($D \neq 0$) is the clean (dirty) limit. The vertical green (gray) line is the T-range emphasized here: at T_c, long-range order develops, and at T^* SC clusters (short-range order) are formed. In practice, the AF → SC transition is reached in Eq. (1) by decreasing ρ_{SC} from zero, favoring SC, and decreasing $\rho_{\mathrm{AF}} > 0$, reducing AF, for example, by fixing the relation $\rho_{\mathrm{AF}} = 1 + \rho_{\mathrm{SC}}$ [8]. The disorder in the couplings is *correlated* with power $\alpha = 0.8$ [17]. (b) SC correlation (SS) vs T at short [vectorial distance (3,0)] and long [vectorial distance (16,16)] distance, in the clean and dirty limits. Results are from MC simulations on a 32×32 cluster with periodic boundary conditions, using 2000 (3000) thermalization (measurement) steps, starting with a random initial configuration. ρ_{SC} was taken from a bimodal distribution with values -1.1 and -0.1 in the dirty limit, and uniformly -1.1 in the clean limit. SS is defined as $SS(\mathbf{i}) = \frac{1}{N_{\mathrm{sites}}}\sum_{\mathbf{j}}|\Delta_{\mathbf{j}}||\Delta_{\mathbf{j}+\mathbf{i}}|\cos(\phi_{\mathbf{j}} - \phi_{\mathbf{j}+\mathbf{i}})$. Some results gathered on 64×64 lattices show that size effects are not important. (c) Classical SC order parameter Δ for a typical MC-equilibrated configuration at several T's (0.2, $1.0 \sim T_c$, 1.5 and $2.0 \sim T^*$). Color intensity (shades of gray) represents $\langle\Delta\rangle$ averaged over short MC times, and the actual colors (shades of gray) represent the SC angle ϕ at each site (see wheel). The maximum value of $|\Delta|$ for the temperatures studied was ~2.0. The bimodal couplings configuration is also shown (d): blue (dark gray) is where SC dominates ($\rho_{\mathrm{SC}} = -1.1$); red (light gray) where AF dominates ($\rho_{\mathrm{SC}} = -0.1$).

$$H_{\mathrm{F}} = -t\sum_{\langle\mathbf{ij}\rangle,\sigma}(c^{\dagger}_{\mathbf{i}\sigma}c_{\mathbf{j}\sigma} + \mathrm{H.c.}) + 2\sum_{\mathbf{i}}J_{\mathbf{i}}S^z_{\mathbf{i}}s^z_{\mathbf{i}} + \frac{1}{2}\sum_{\mathbf{i},\alpha}V_{\mathbf{i}}|\Delta_{\mathbf{i}\alpha}|^2 - \sum_{\mathbf{i},\alpha}V_{\mathbf{i}}(\Delta_{\mathbf{i}\alpha}c_{\mathbf{i}\uparrow}c_{\mathbf{i}+\alpha\downarrow} + \mathrm{H.c.}), \quad (2)$$

where $c_{\mathbf{i}\sigma}$ are fermionic operators, $s^z_{\mathbf{i}} = (n_{\mathbf{i}\uparrow} - n_{\mathbf{i}\downarrow})/2$, $n_{\mathbf{i}\sigma}$ is the number operator, and $\Delta_{\mathbf{i}\alpha} = \beta|\Delta_{\mathbf{i}}|e^{i\phi_{\mathbf{i}}}$ are complex

numbers for the SC order parameter defined now at the links $(\mathbf{i}, \mathbf{i}+\alpha)$ [α = unit vector along the x or y directions; to account for the d-wave nature of the SC state, we use $\beta = 1\,(-1)$ for α along x (y)]. For each $\{\Delta_{\mathbf{i}\alpha}\}$ and $\{S^z_{\mathbf{i}}\}$ configuration generated by the LG/MC procedure, the fermionic sector is simply exactly diagonalized via library subroutines (no extra MC steps are needed since the order-parameters background is here assumed fixed) and any property, static or dynamic, can be easily obtained. At $J_{\mathbf{i}} = 0$, d-wave SC is favored since the pairing term involves NN sites [11]. The parameters of relevance are $J_{\mathbf{i}}$ and $V_{\mathbf{i}}$ (t is the energy unit), and they carry a site dependence to easily include quenched disorder [12].

Fermi arcs.—Figure 2 contains our most important results. (a) shows the one-particle spectral function $A(\mathbf{k}, \omega)$ along a straight N-AN line. At low $T < T_c$, the d-wave SC gap is clearly visible [13]. However, as T is raised first across T_c, then through the intermediate SCCS phase-fluctuating regime, and finally to above T^*, the gaps disappear forming segments (arcs) starting at the node, with a length that grows with increasing T. In (b), the FS's are shown: four nodes at low T become arcs at higher T; they eventually merge and form a closed FS. (c) contains an example of gaps vs $\mathbf{k}$ along the N-AN line, showing the arc formation and the stability of the AN gap even varying T over a wide range. Here, as in [3,4], a given $\mathbf{k}$ is said to have a gap if two peaks are found in $A(\mathbf{k}, \omega)$. In Fig. 3(a), the length of the Fermi arc is shown vs T, and an approximate linear relation is found. All these results are in agreement with ARPES [3,4,14].

The arcs are *not* merely caused by the broadening of the peaks by disorder. To understand this, consider now the direction *perpendicular* to the N-AN line. In Fig. 2(d), $A(\mathbf{k}, \omega)$ from $(0, \pi/2)$ to $(\pi/2, \pi)$ is shown. This crosses the N-AN line at $(\pi/4, 3\pi/4)$. In the range $T_c < T < T^*$, a *metallic* dispersion, close to noninteracting electrons, is observed. This is different from the low-T results that show a Bogoliubov–de-Gennes (BdG) quasiparticle dispersion and a gap (also shown). Monitoring the LDOS, we also noticed the existence of gapless metallic patches

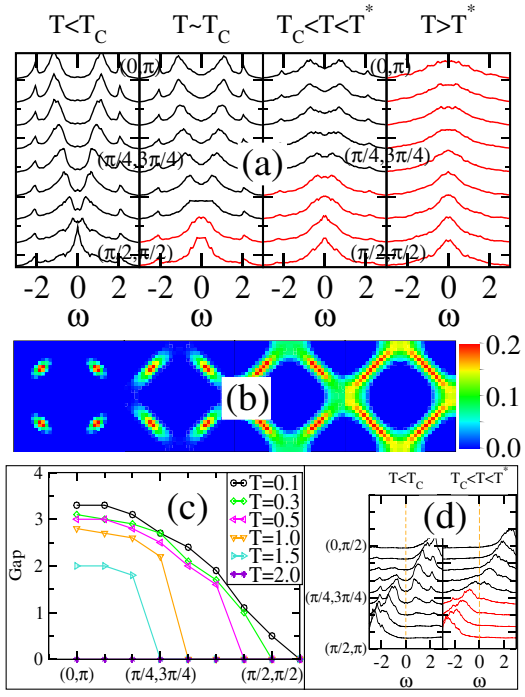

FIG. 2 (color online). (a) $A(\mathbf{k}, \omega)$ for equally spaced $\mathbf{k}$'s along the direction from $(\pi/2, \pi/2)$ (bottom) to $(0, \pi)$ (top). The classical LG configurations used are obtained as described in Fig. 1 but for the case $\rho_{SC} = -0.8$ (0) in the SC (AF) regions, using $\rho_{AF} = 1 + \rho_{SC}$, on a 32×32 lattice. The T's are, from left to right, $T = 0.1$, 0.4, 1.0, and 2.0. In this case, $T_c \sim 0.4$, and $T^* \sim 1.2$–1.5. (b) $A(\mathbf{k}, \omega = 0)$ in the $k_x - k_y$ plane for the same parameters and temperatures as in (a). Results shown are those within a window $\Delta\epsilon = 0.1$ from the Fermi level. (c) SC gap (distance between peaks) vs momentum for the same parameters as in (a) but with $\rho_{SC} = -1.1$ or -0.1 (bimodal distribution), at the T's indicated. (d) $A(\mathbf{k}, \omega = 0)$ from $(0, \pi/2)$ to $(\pi/2, \pi)$, at $T = 1.0$ and 0.1, and parameters as in (a).

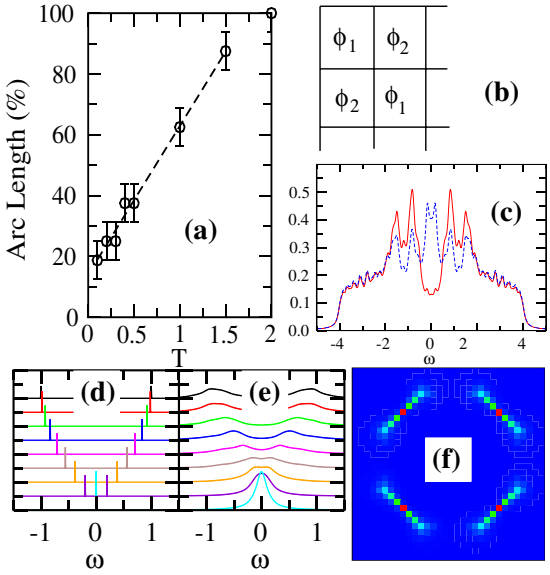

FIG. 3 (color online). (a) Length of the Fermi arc (as a % of the maximum length) vs T for the case described in Fig. 2(a). The Fermi arc was defined to exist at a certain momentum $\mathbf{k}$ when its intensity was within 35% of the maximum intensity. Other definitions lead to a similarly linear relation but with different $T \to 0$ limits. The energy cutoff $\Delta\epsilon = 0.1$ prevent the size of the nodes from being exactly zero in the low-T state. (b) Schematic representation of the toy model configuration (see text). ϕ_1 and ϕ_2 refer to the SC order parameter phases in 4×4 squares. (c) LDOS for the example shown in (b) with $\phi_1 = 0$ and $\phi_2 = \pi$. The red (solid) line corresponds to a site at the center, and the blue (dashed) line to a site on the (border) of the 4×4 square. The parameters used are the same at each site: $|\Delta| = 1$, $V = 0.25$, and $J = 2$. (d) $A(\mathbf{k}, \omega)$ for $\mathbf{k}$ along the direction $(\pi/2, \pi/2)$ to $(0, \pi)$ for the case shown in (b) with $\phi_1 = \phi_2 = 0$ (i.e., perfect d-wave superconductor). (e) Same as (d), but with ϕ_1 and ϕ_2 randomly chosen between 0 and π. (f) $A(\mathbf{k}, \omega = 0)$ in the $k_x - k_y$ plane for case (e) ($\Delta\epsilon = 0.1$).

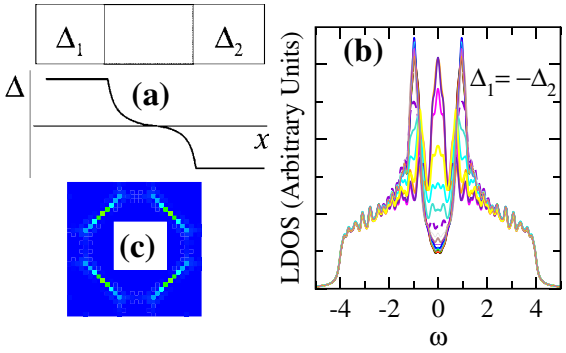

FIG. 4 (color online). (a) Schematic representation of a Josephson-junction-like structure. *Top*: two SC regions with order parameters Δ_1 and Δ_2, separated by a $\Delta = 0$ area of width w (gray). *Bottom*: expected gap interpolation for $\Delta_1 = -\Delta_2$. (b) LDOS on a 32×32 lattice containing 4 equally-spaced 12×12 SC clusters separated by $w = 4$. The order parameters are staggered between clusters using $\Delta_1 = 1$ and $\Delta_2 = -1$, with $V = 0.25$ and without AF ($J = 0$). Shown are results from the center of one SC region to a nearest neighbor. (c) $A(\mathbf{k}, \omega = 0)$ in the $k_x - k_y$ plane for $\Delta_1 = -\Delta_2 = 1$ and $w = 2$, with a setup as described in (b) but using 14×14 SC clusters.

coexisting with the AF and SC clusters. These metallic regions appear in ''fragile'' zones of the disordered configuration, i.e., long and thin areas of one phase penetrating into the other, where none of the two orders prevails. Thus, the SCCS actually involves three ingredients: SC, AF, and metallic areas. The metallic areas and Fermi arcs appear related.

Toy models.—To better understand the Fermi arc formation in the SCCS, consider a 2D square lattice regularly divided into smaller 4×4 squares [Fig. 3(b)], all with the same SC amplitude but different phases, and without AF. To simulate T effects, frozen configurations $\{\phi\}$ of the SC phases were studied. In Fig. 3(d), the uniform case $\phi_1 = \phi_2 = 0$ is shown and a clear d-wave gap exists along the N-AN line. This mimics the regime $T < T_c$ in Fig. 2(a). To simulate $T_c < T < T^*$, consider now a *random* distribution of phases. The result [Fig. 3(e)] still shows a clear gap in the AN point, but near the nodal point, now a finite set of momenta do *not* present a gap anymore, generating a Fermi arc [see also the FS in Fig. 3(f)]. In general, we observed that angles with $\cos(\phi_2) < 0$ contribute the most to the arcs [see Fig. 3(c)] [15]. The metallic density-of-states has a van Hove singularity in 2D.

Relevance of large phase differences.—Consider Fig. 4(a): here two SC clusters are shown, with order parameters $\Delta_1 \neq 0$ and $\Delta_2 \neq 0$, separated by an intermediate thin region where $\Delta = 0$. If $\Delta_1 = \Delta_2$, this intermediate region will develop a gap by proximity effect, and the FS has still 4 nodes, as confirmed by an explicit BdG calculation (not shown). However, if $\Delta_1 = -\Delta_2$, a qualitative difference occurs: now the interpolation in the intermediate region necessarily requires the existence of a *zero*, where the SC order parameter must vanish even for a thin $\Delta = 0$ layer [Fig. 4(a)]. A BdG study confirms that the LDOS in the middle between two ''antiparallel'' SC clusters is similar to the LDOS of a metallic state [see Fig. 4(b)]. The FS for $\Delta_1 = -\Delta_2$ has Fermi arcs [Fig. 4(c)]. Large ϕ differences induce metallic regions, that cause the Fermi arcs.

Conclusions.—A state based on SC clusters with random phases was used to calculate the photoemission response. Fermi arcs were found in a T range between T_c and the T^* where the clusters start forming upon cooling. This T^* is expected to be similar to the PG critical temperature at hole doping concentrations where superconductivity is found at low T [16].

Work supported by the NSF Grant No. DMR-0706020, the Div. of Mat. Science and Eng., U.S. DOE, under contract with UT-Battelle, LLC, and by the CNMS, sponsored by the Scientific User Facilities Div., BES-DOE.

[1] A. Damascelli *et al.*, Rev. Mod. Phys. **75**, 473 (2003).
[2] M. Norman *et al.*, Nature (London) **392**, 157 (1998).
[3] A. Kanigel *et al.*, Nature Phys. **2**, 447 (2006).
[4] A. Kanigel *et al.*, Phys. Rev. Lett. **99**, 157001 (2007).
[5] K. Gomes *et al.*, Nature (London) **447**, 569 (2007).
[6] This is compatible with Nernst experiments [Y. Wang *et al.*, Phys. Rev. B **73**, 024510 (2006)], and μ-SR measurements: J. Sonier *et al.*, Phys. Rev. Lett. **101**, 117001 (2008).
[7] M. Randeria *et al.*, Phys. Rev. Lett. **69**, 2001 (1992); V. J. Emery and S. A. Kivelson, Nature (London) **374**, 434 (1995); Z. Tesanovic, Nature Phys. **4**, 408 (2008).
[8] G. Alvarez *et al.*, Phys. Rev. B **71**, 014514 (2005); M. Mayr *et al.*, Phys. Rev. B **73**, 014509 (2006).
[9] In practice, following [8], we used $r_{SC} = -1$, $r_{AF} = -0.85$, $u_{SC} = u_{AF} = 1$, and $u_{SC|AF} = 0.7$
[10] Calculations have been repeated for several configurations, and they are all qualitatively similar.
[11] At $T \to 0$, the BdG equations with a competing AF interaction are recovered. The chemical potential is $\mu = 0$ (density $n = 1$) for both the AF and SC clusters.
[12] We chose $V = -0.25\rho_{SC}$ (0) where $\rho_{SC} < 0 (> 0)$. Reciprocally, $J = 2.0\rho_{AF}$ (0) if $\rho_{AF} > 0$ (< 0).
[13] Higher $|\omega|$ peaks are related with a nodeless AF gap, and they do not affect lower energy features. See also T. Das *et al.*, Phys. Rev. B **77**, 134516 (2008); **77**, 219904 (2008).
[14] Fermi arcs were also obtained in E. Berg and E. Altman, Phys. Rev. Lett. **99**, 247001 (2007).
[15] See also A. Martin and J. Annett, arXiv:cond-mat/9910208.
[16] However, as shown in Ref. [8], for dopings very close to half filling, the PG becomes dominated by the AF state. Thus, the AF clusters must also be considered for an understanding of the full doping regime.
[17] H. Makse *et al.*, Phys. Rev. E **53**, 5445 (1996).